

# Illumination-based Transformations Improve Skin Lesion Segmentation in Dermoscopic Images

Kumar Abhishek, Ghassan Hamarneh, and Mark S. Drew  
School of Computing Science, Simon Fraser University, Canada

Email: [kabhishe@sfu.ca](mailto:kabhishe@sfu.ca)



# Introduction



# Clinical motivation

- Cancer is the second leading cause of death globally.
  - 1 out of every 6 deaths is cancer-related.
- Skin cancer is the most prevalent cancer globally.
  - Estimated 5 million cases will be diagnosed in 2020 in USA alone.
- Incidence rate of skin cancer increasing in the past decades [WHO, 2020].
- The early detection, diagnosis, and treatment of skin cancers is extremely important.
  - The estimated five-year survival rate of skin cancers with early detection is about **99%** [Siegel et al., Cancer Statistics, 2020].



# Computer Aided Diagnosis of Skin Lesions

## Advantages:

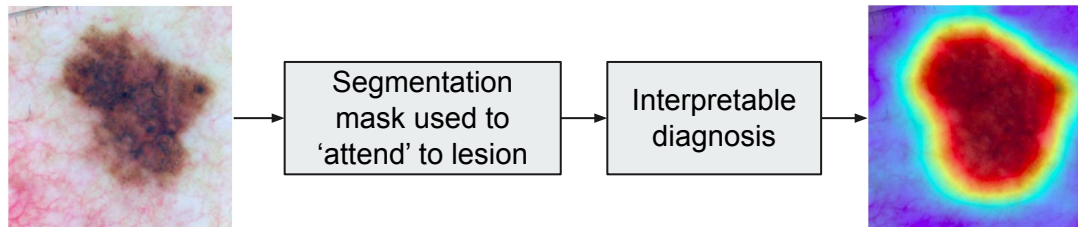
- Quick, robust, and reproducible results to assist dermatological diagnoses.
  - Able to serve as the source of a second opinion.
- Reduced diagnostic costs.
- Alleviate the lack of dermatological expertise in underserved communities through teledermatology.

# Skin Lesion Segmentation

Localizing the lesion is often the first step in diagnosis.

Segmentation provides an added sense of trust in automated diagnosis algorithms.

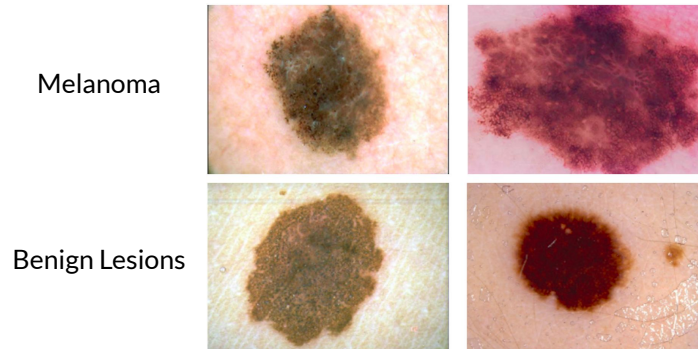
Lesion segmentation localizes region for information extraction.



# Motivation

Deep learning based segmentation approaches usually ignore illumination and color based knowledge.

“changes in the acquisition setup can **alter the colors of an image**. ... The human brain is able to **compensate for this variability**, but the same cannot be said of a CAD system” [Barata et al., ICIP 2014]





# Motivation

Very few works have explored color constancy algorithms and used multiple color space representations for skin lesion segmentation.

**Goal:** Leverage knowledge about illumination and skin imaging in a deep learning-based segmentation model.



# Method





# Selecting Color Channels

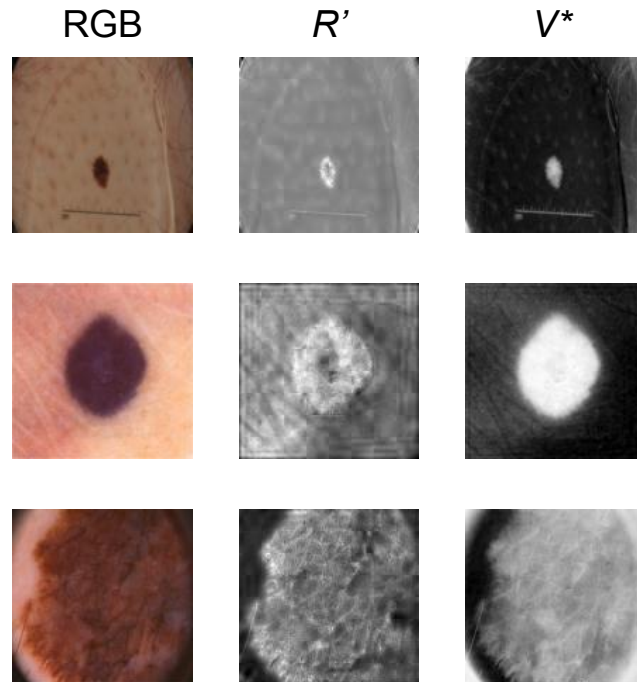
“the normalized RGB space eliminates the effect of varying intensities due to uneven illumination and it is free from shadow and shading effects” [Guarracino et al., JBHI 2019]

Two color channels selected:

- Red channel from normalized RGB image (denoted by  $R'$ )
- Complement of value channel ( $V$ ) from HSV color space representation (denoted by  $V^*$ ).

$$R' = \frac{R}{R + G + B} \quad V^* = 1 - V \quad V = \max\left(\frac{R}{M}, \frac{G}{M}, \frac{B}{M}\right)$$

# Selecting Color Channels: Results



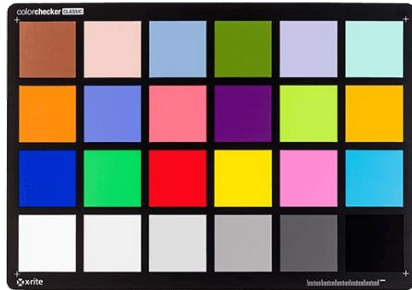


# Intrinsic Images

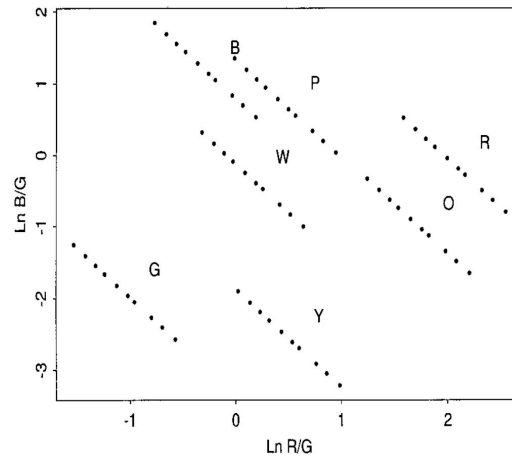
**Motivation:** Shadows in images can cause automated algorithms (including segmentation methods) to fail.

**Goal:** Find an illumination-invariant 'intrinsic' image of a scene that depends only on the reflectance properties.

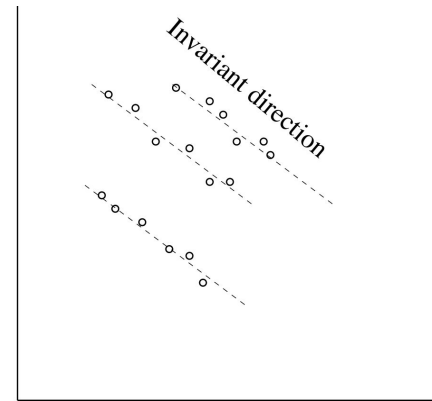
# Intrinsic Images Using Camera Calibration



Color checker



2D log chromaticity plots for 7 patches imaged under 10 illuminants



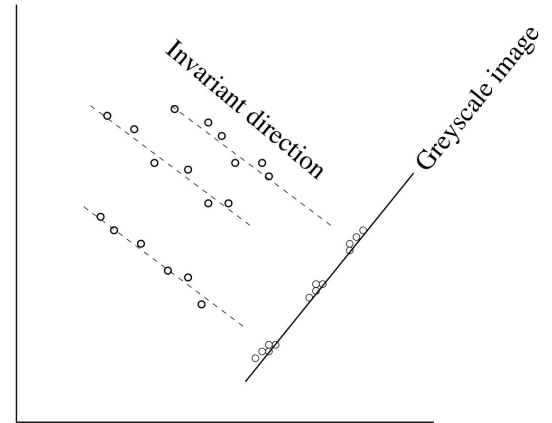
Finding the invariant direction

# Intrinsic Images

This process is camera dependent.

**Goal:** Find the invariant direction without imaging the scene with more than one illuminant.

Invariant direction = direction along which the projected image has minimum entropy.



# Intrinsic Images: Overview



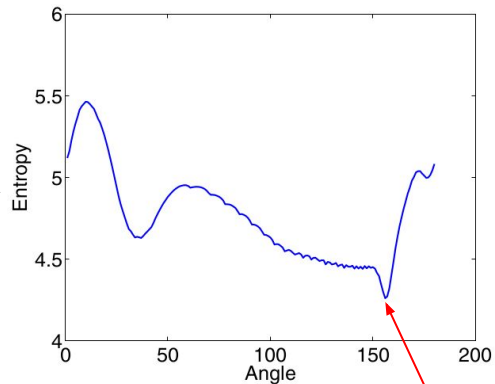
RGB Image



2D log chromaticity

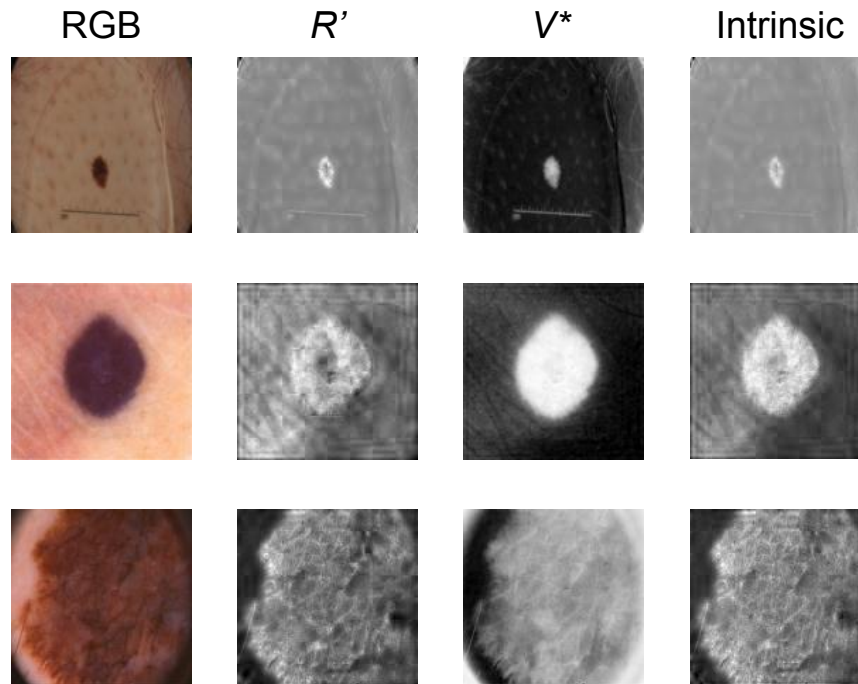


Calculate entropy for angles from  $0^\circ$  to  $180^\circ$



Intrinsic Image

# Intrinsic Images: Results





# Grayscale Images of Skin Lesions

**Goal:** Find a single channel (grayscale) representation of the skin lesion image based on optics of the human skin.

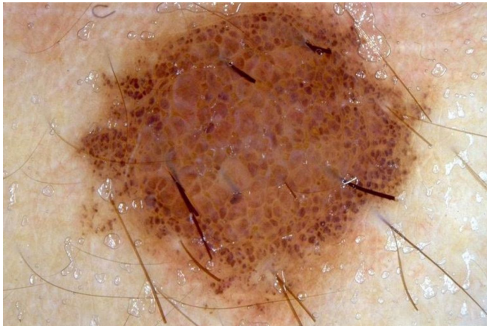
Consider the optical density space:  $[-\log R, -\log G, -\log B]$ .

In this space, RGB value triplets for pixels in skin images reside on a plane [Tsumura et al., JOSAA 1999].

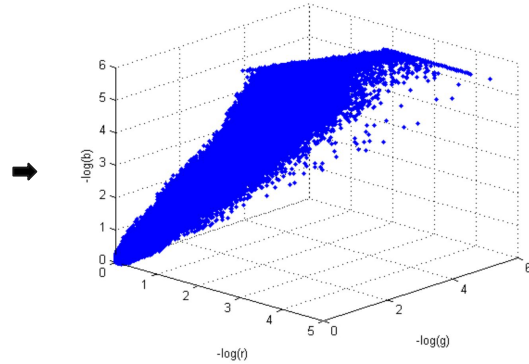
“by carrying PCA, eigenvalues indicate that the data is **distributed mostly along a vector** (rather than a plane)” [Madooei et al., CIC 2012].



# Grayscale Images of Skin Lesions



Skin lesion RGB image

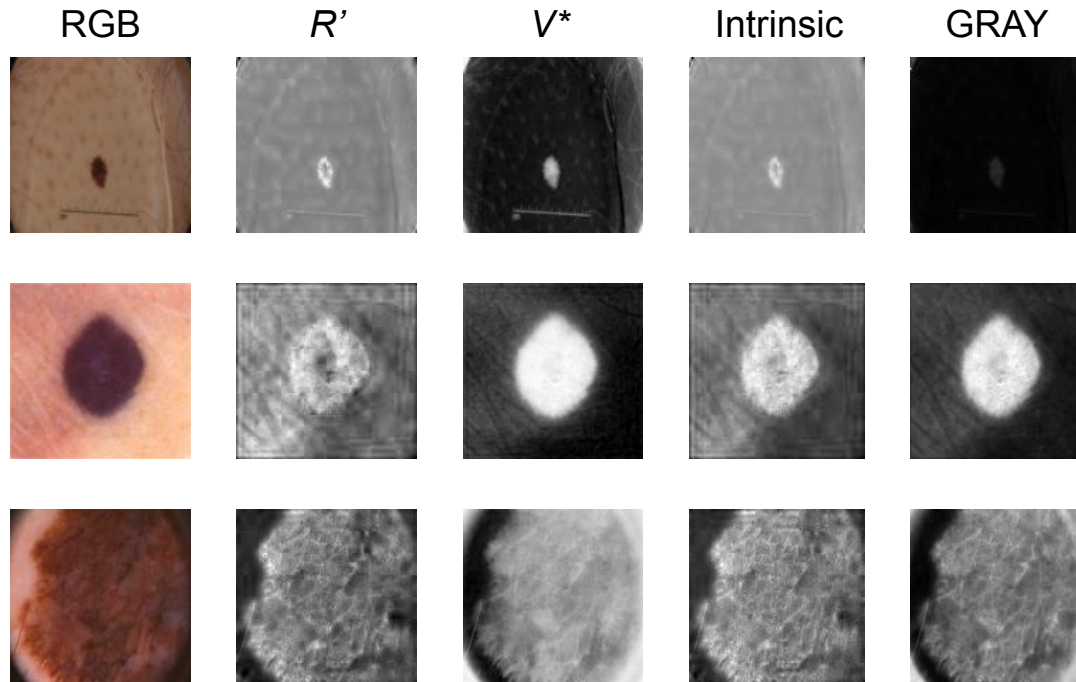


Optical density space representation

PCA

98.3% total variance explained by 1<sup>st</sup> principal component

# Grayscale Images of Skin Lesions: Results





# Shading-attenuated Images

**Motivation:** Imaging non-flat skin surfaces, especially lesions, can induce shading in dermoscopic images, which can degrade the segmentation.

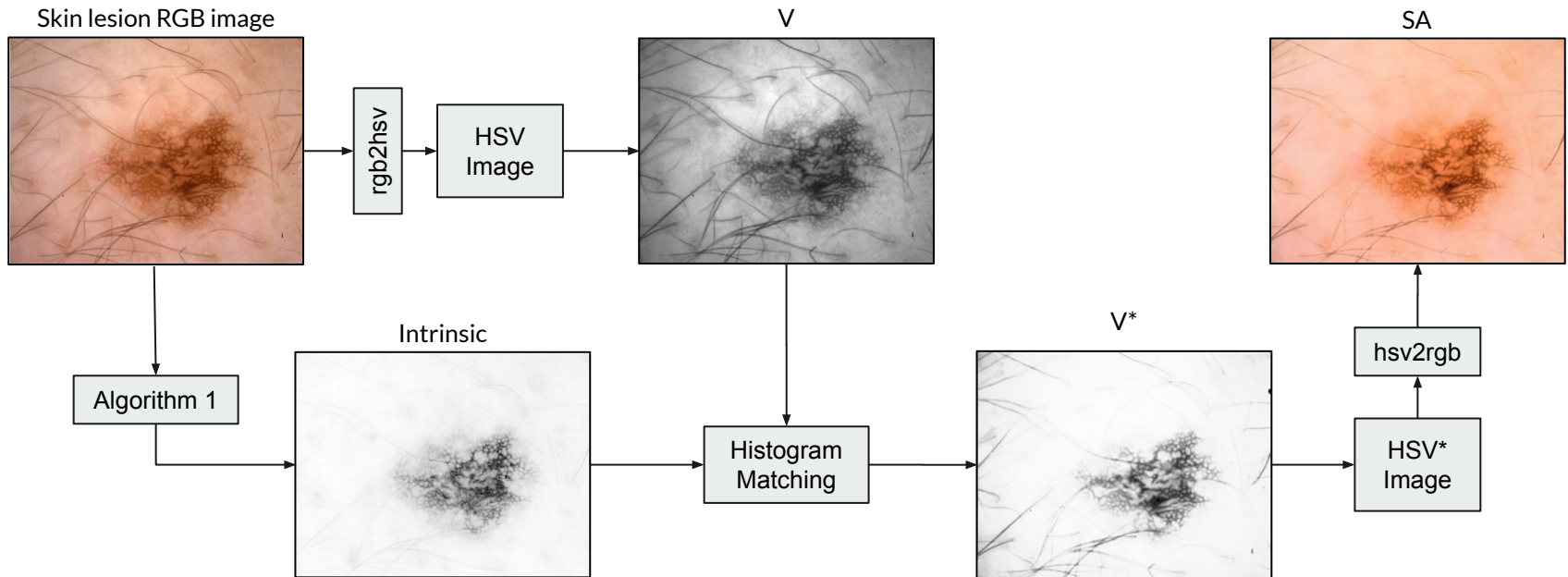
**Goal:** Attenuate shading in dermoscopic images.

Normalize illumination w.r.t the intrinsic image [Madooei et al., CIC 2012]

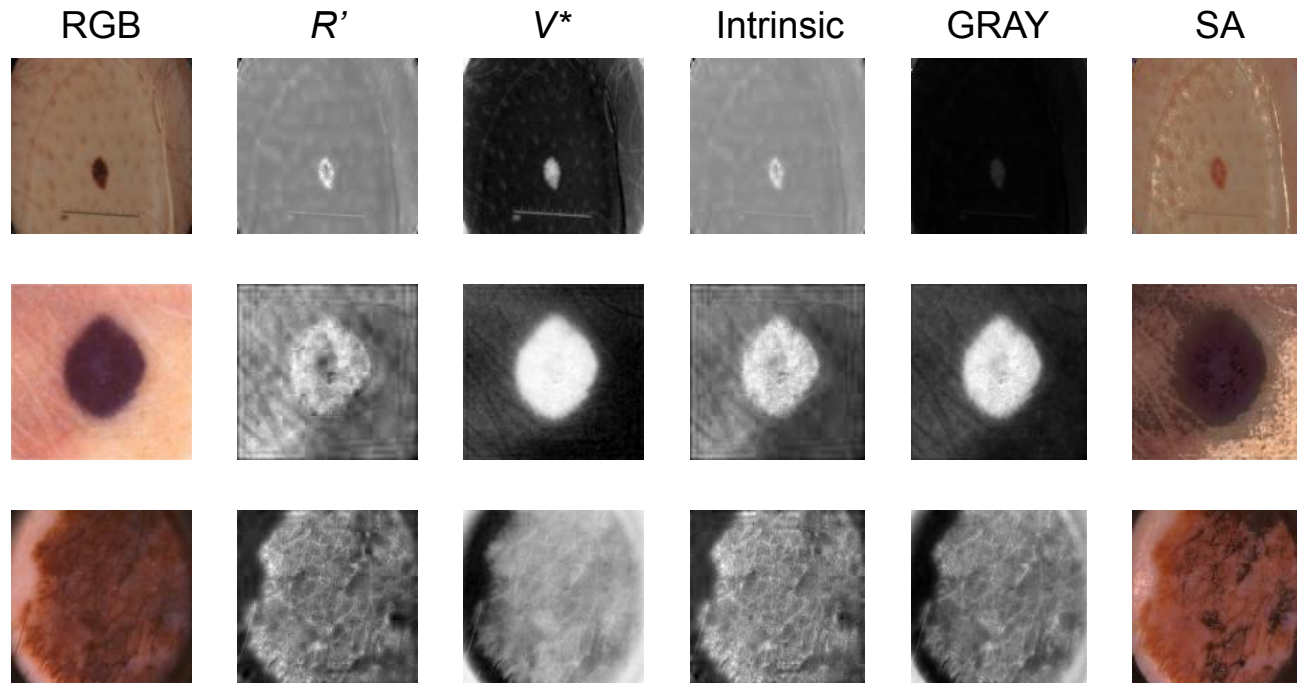
**Illumination:** V channel from HSV color space representation.

The shading effects are visible in the V channel [Soille et al., 1999]

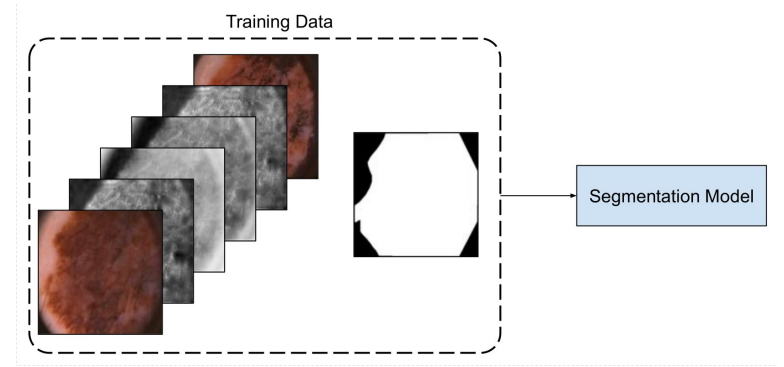
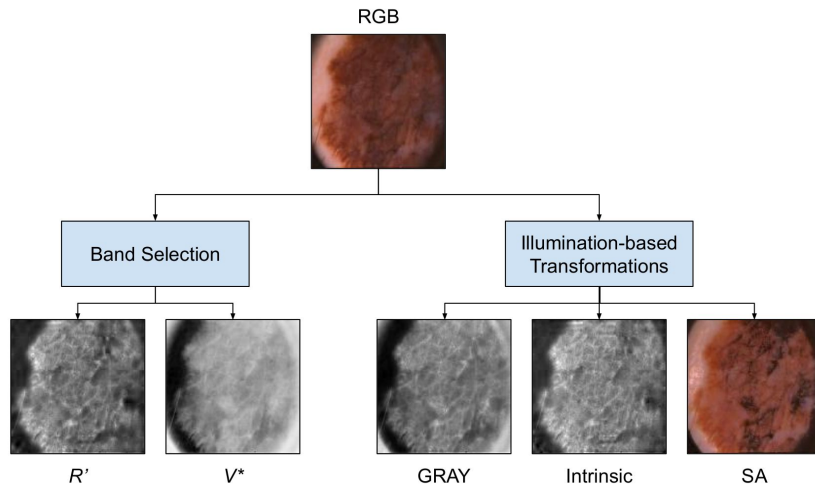
# Shading-attenuated Images: Overview



# Shading-attenuated Images: Results



# Method Overview





# Datasets, Experiments, and Results



# Datasets

3 datasets used

DermoFit split into training:validation:testing partitions in 60:10:30 ratio.

PH2 used entirely for testing.

<b>Split</b>	Training	Validation	Testing
<b>Dataset</b>			
ISIC 2017	2000	150	600
DermoFit	1300	-	-
PH2	200	-	-





# Evaluation: Ablation Study

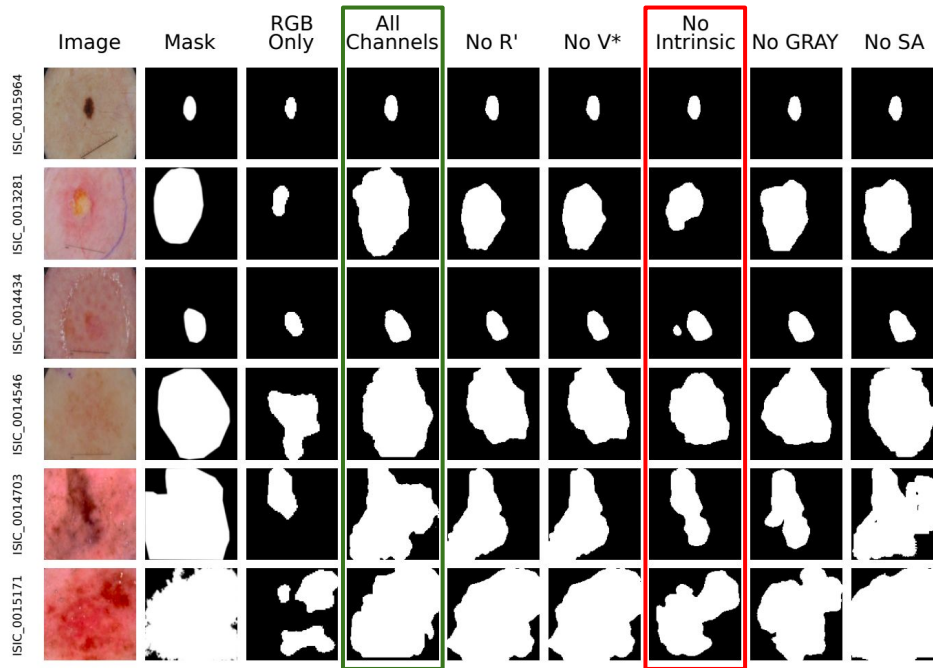
7 models trained and evaluated on the ISIC 2017 dataset with the following inputs to the networks:

- RGB images only ('RGB Only')
- RGB + all transformation based channels ('All Channels')
- Drop one transformation at a time from 'All Channels':
  - Call it 'No x', where  $x \in \{R, V^*, \text{Intrinsic}, \text{GRAY}, \text{SA}\}$
  - 5 such models.

## Ablation Study: Quantitative Results

Method	Accuracy	Dice Coefficient	Jaccard Index	Sensitivity	Specificity
RGB Only	$0.9029 \pm 0.0053$	$0.7781 \pm 0.0086$	$0.6758 \pm 0.0095$	$0.7471 \pm 0.0091$	$0.9683 \pm 0.0031$
All Channels	<b><math>0.9220 \pm 0.0045</math></b>	<b><math>0.8386 \pm 0.0078</math></b>	<b><math>0.7570 \pm 0.0089</math></b>	<b><math>0.8706 \pm 0.0077</math></b>	$0.9516 \pm 0.0037$
No $R'$	$0.9185 \pm 0.0046$	$0.8243 \pm 0.0078$	$0.7363 \pm 0.0090$	$0.7949 \pm 0.0085$	$0.9735 \pm 0.0030$
No $V^*$	$0.9189 \pm 0.0049$	$0.8263 \pm 0.0077$	$0.7381 \pm 0.0089$	$0.7892 \pm 0.0087$	$0.9786 \pm 0.0025$
No Intrinsic	$0.9092 \pm 0.0056$	$0.7997 \pm 0.0094$	$0.7139 \pm 0.0103$	$0.7662 \pm 0.0104$	<b><math>0.9803 \pm 0.0024</math></b>
No GRAY	$0.9116 \pm 0.0052$	$0.8163 \pm 0.0080$	$0.7260 \pm 0.0091$	$0.8041 \pm 0.0090$	$0.9643 \pm 0.0033$
No SA	$0.9198 \pm 0.0050$	$0.8274 \pm 0.0083$	$0.7445 \pm 0.0093$	$0.8137 \pm 0.0088$	$0.9603 \pm 0.0044$

# Ablation Study: Qualitative Results





## Evaluation on other datasets: DermoFit and PH2

2 models trained on the DermoFit dataset with the following inputs to the networks:

- RGB Only
- No SA

No SA used because SA images do not contribute much to performance improvement and are somewhat computationally expensive.

Both models evaluated on DermoFit and PH2 datasets.



# Quantitative Results

Dataset	Method	Accuracy	Dice Coefficient	Jaccard Index	Sensitivity	Specificity
DermoFit	RGB Only	$0.9024 \pm 0.0038$	$0.8437 \pm 0.0053$	$0.7418 \pm 0.0069$	$0.8080 \pm 0.0078$	<b><math>0.9534 \pm 0.0030</math></b>
	No SA	<b><math>0.9124 \pm 0.0030</math></b>	<b><math>0.8674 \pm 0.0042</math></b>	<b><math>0.7737 \pm 0.0055</math></b>	<b><math>0.8721 \pm 0.0053</math></b>	$0.9347 \pm 0.0032$
PH2	RGB Only	$0.8546 \pm 0.0133$	$0.7989 \pm 0.0128$	$0.6944 \pm 0.0140$	$0.8032 \pm 0.0166$	$0.9543 \pm 0.0031$
	No SA	<b><math>0.8926 \pm 0.0091</math></b>	<b><math>0.8537 \pm 0.0071</math></b>	<b><math>0.7559 \pm 0.0091</math></b>	<b><math>0.8442 \pm 0.0110</math></b>	<b><math>0.9607 \pm 0.0022</math></b>



# Summary

- Motivated by information from illumination and skin imaging, we proposed a segmentation framework to incorporate certain color bands and illumination-based transformations.
- Our experiments on multiple datasets show the potential value of using such information to improve segmentation.
- An ablation study demonstrates the relative importance of various transformations.
- It is unclear why the deep segmentation model trained on RGB images only cannot learn to generate these transformations.
  - Future work: attempt to learn to estimate these illumination-based transformations in a deep learning setting.



# References

- WHO | Cancer, <https://www.who.int/news-room/fact-sheets/detail/cancer>, 2020.
- Rebecca L. Siegel et al., “Cancer Statistics, 2020”. *CA: A Cancer Journal for Clinicians*, 2020.
- Yiqi Yan et al., “Melanoma recognition via visual attention”, *Lecture Notes in Computer Science*, 2019.
- Giuseppe Argenziano et al., “Interactive atlas of dermoscopy (book and CD-ROM)”, 2000.
- Catarina Barata et al., “Improving dermoscopy image analysis using color constancy”, *ICIP*, 2014.
- Jia hua Ng et al., “The effect of color constancy algorithms on semantic segmentation of skin lesions”, *SPIE Medical Imaging*, 2019.
- Yading Yuan, “Automatic skin lesion segmentation with fully convolutional-deconvolutional networks”, *arXiv:1703.05165*, 2017.
- Graham D Finlayson et al., “Intrinsic images by entropy minimization”, *European Conference on Computer Vision*, 2004.
- Mario Rosario Guarracino et al., “SDI+: A novel algorithm for segmenting dermoscopic images”, *IEEE Journal of Biomedical and Health Informatics*, 2018.
- Norimichi Tsumura et al., “Independent-component analysis of skin color image”, *Journal of the Optical Society of America A*, 1999.
- Ali Madooei et al., “Automated pre-processing method for dermoscopic images and its application to pigmented skin lesion segmentation”, *Color and Imaging Conference*, 2020.
- Pierre Soille, “Morphological Operators”, *Handbook of Computer Vision and Applications*, 1999.



Thank you.

[www.MedicalImageAnalysis.com](http://www.MedicalImageAnalysis.com)

## Acknowledgements



compute | calcul  
canada | canada

